Diffusion-limited reactions in crowded environments: a local density approximation

2013 J. Phys.: Condens. Matter 25 375104

(http://iopscience.iop.org/0953-8984/25/37/375104)

J. Phys.: Condens. Matter **25** (2013) 375104 (10pp) doi:10.1088/0953-8984/25/37/375104

Diffusion-limited reactions in crowded environments: a local density approximation

F Piazza[1], N Dorsaz[2], C De Michele[3], P De Los Rios[4] and G Foffi[5,6]

[1] Centre de Biophysique Moléculaire (CBM), CNRS UPR 4301, Rue Charles Sadron, F-45071 Orléans, France
[2] Department of Chemistry, University of Cambridge, Lensfield Road, Cambridge CB2 1EW, UK
[3] Dipartimento di Fisica, 'Sapienza' Universit di Roma, Piazzale Aldo Moro 2, I-00185, Roma, Italy
[4] Ecole Polytechnique Fédérale de Lausanne (EPFL), Institute of Theoretical Physics, Laboratory of Statistical Biophysics, 1015 Lausanne, Switzerland
[5] Ecole Polytechnique Fédérale de Lausanne (EPFL), Institute of Theoretical Physics, 1015 Lausanne, Switzerland
[6] Laboratoire de Physique de Solides, UMR 8502, Bâtiment 510, Universit é Paris-Sud, F-91405 Orsay, France

E-mail: Francesco.Piazza@cnrs-orleans.fr and giuseppe.foffi@epfl.ch

Received 6 March 2013, in final form 24 July 2013
Published 21 August 2013
Online at stacks.iop.org/JPhysCM/25/375104

Abstract
In the real world, diffusion-limited reactions in chemistry and biology mostly occur in crowded environments, such as macromolecular complex formation in the cell. Despite the paramount importance of such phenomena, theoretical approaches still mainly rely on the Smoluchowski theory, only valid in the infinite dilution limit. In this paper we introduce a novel theoretical framework to describe the encounter rate and the stationary density profiles for encounters between an immobilized target and a fluid of interacting spherical particles, valid in the local density approximation. A comparison with numerical simulations performed for a fluid of hard spheres and square well attractive hard spheres confirms the accuracy of our treatment.

(Some figures may appear in colour only in the online journal)

1. Introduction

Binding of different molecules, or their absorption by specific substrates, needs first the different molecular components to encounter by diffusive motion, and subsequently the specific reaction to take place within the encounter complex [1]. In solution the latter part of the process typically proceeds much faster than the former, and the reaction is thus overall limited by diffusion. Because diffusion-limited reactions are common in biology and chemistry, a complete characterization of the formation of the encounter complex is a key step towards their understanding. The simplest theory for a reaction of the type

$$\mathrm{A} + \mathrm{B} \rightarrow \mathrm{B} \tag{1}$$

was proposed almost a century ago by Smoluchowski in terms of two isotropically reactive diffusing spherical molecules A and B, that diffuse until they meet, yielding the encounter complex [2]. At low concentrations, and for $D_\mathrm{A} \gg D_\mathrm{B}$, one can work in the reference frame where a B particle is at rest and tracers diffuse with an effective diffusion constant $D = D_\mathrm{A} + D_\mathrm{B}$, which is akin to the Born–Oppenheimer approximation made in solid-state physics [3]. This setting is known as the target problem, as opposed to the trapping problem, where a single test particle diffuses in the presence of a static, quenched distribution of absorbers (traps). We note that, while in the infinite dilution limit the two problems obviously coincide, a full quantitative picture of how many-body effects due to inter-particle interactions influence the A–B encounter is still lacking.

The encounter takes place when the centres of the two molecules are at a distance $R = a+b$, the sum of the individual radii a and b. In the infinite dilution limit, one can reformulate

the many-body problem in terms of a two-body problem. The governing equation of the process is then

$$\frac{\partial \rho(\vec{r},t)}{\partial t} = D\nabla^2 \rho(\vec{r},t) \tag{2}$$

where $\rho(\vec{r},t)$ is the local density of molecules at time t. Equation (2) has to be solved with boundary conditions

$$\text{(i)}\ \rho(\vec{r},t)|_{|\vec{r}|=R} = 0 \qquad \text{(ii)}\ \lim_{|\vec{r}|\to\infty} \rho(\vec{r},t) = \rho_\infty \tag{3}$$

implementing (i) the irreversible formation of the encounter complex, and thus the loss of a tracer A molecule, and (ii) fixing the tracer bulk concentration ρ_∞ (that is, the concentration far from B molecules). In spherical coordinates, equation (2) has the simple stationary solution

$$\rho(\vec{r}) = \rho_\infty \left(1 - \frac{R}{r}\right). \tag{4}$$

Correspondingly, the rate of encounter complex formation, that is, the overall flux across the sink surface, reads

$$\kappa_S = 4\pi D R \rho_\infty. \tag{5}$$

Equations (2) and (3) describe the encounter process in the ideal case of infinite dilution $\rho_\infty \to 0$.

In real-world situations, diffusion-limited reactions take place in crowded environments, such as the cell, and interactions between the diffusing particles cannot be neglected. As a consequence, the encounter dynamics must be treated as a many-body process.

The effect of macromolecular crowding has been discussed in several contexts, such as association, isomerization, protein folding and stability with respect to denaturation. Several critical reviews have been published in the last years and we direct the reader to them for an exhaustive overview of the field [4–6]. Concerning the development of theoretical and computational tools, the use of coarse-grained schemes, where the crowding agents are often modelled as ideal or quasi-ideal spheres (HS), has proven quite useful.

This allows the use of simple thermodynamics arguments, where scaled particle theory is used for the calculation of the free-energy of the formation of a cavity in a HS fluid or a fluid of hard ellipsoids [7]. In this framework, simulations have been widely used to determine, for example, the effect of crowding on protein folding [8] and the diffusion in the presence of crowding and hydrodynamic interactions [9].

In the spirit of generalizing Smoluchowski's approach in the simplest possible way, we have recently proposed to consider a reaction of the type presented in equation (1) where the concentration of interacting tracers A is allowed to increase, while the B sinks still form a diluted fluid. This amounts to considering explicitly many-body effects in the target problem. To this end, we have modelled the diffusing tracers of radius a as hard spheres interacting only through their mutual excluded volume and chose the centre of a particle of radius b as our reference frame [10]. Using a novel simulation scheme we have been able to explore the effects of hard-core interactions between particles both on the encounter complex formation rate and on the concentration profiles. More generally, we believe that our approach, borrowing ideas from liquid-state theory and colloidal physics, can represent a promising new direction to explore.

Although simulated experiments represent an extremely powerful tool to investigate the combined consequences of finite concentrations and inter-particle interactions, they must be complemented by a suitable analytical approach to reach a satisfactory understanding. In this paper we derive analytical expressions for the rate and the stationary density profiles within a dynamic density functional theory (DDFT) approach coupled to a local density approximation (LDA). To this aim, we start from the N-body Smoluchowski equation and we arrive to a DDFT formulation of the effective two-body Smoluchowski problem and its solution. To our knowledge, this is the first time that this approach has been laid down for this problem. Our simple LDA approximation makes it possible to go beyond the Smoluchowski regime in the presence of crowding. As a first consistency step, we have re-derived the generalization of the rate constant that we obtained previously using a density-dependent mobility constant [10]. Moreover, the new approach allows us to calculate the stationary density profiles, which can be directly compared with the results of computer simulations. In particular, we derive analytic formulae relating directly the reaction rate and the density profiles to the equation of state (EOS) of the bulk fluid of A particles.

In this paper, we use dynamic Monte Carlo (DMC) simulations for the case of hard spheres and attractive square well particles. For the former, we recover and extend the results of our previous work. For the latter, we show that by choosing an appropriate EOS we can reproduce the rate of reaction quite accurately within the LDA approximation, provided the density is not too large. The generalization towards attractive interactions fits in the wake of several recent observations demonstrating the importance of enthalpic effects in crowded conditions [11–14]. The paper is structured as follows. In section 2, we first derive an effective two-body diffusion equation within the DDFT formalism starting directly from the N-body problem. This derivation has the advantage of defining precisely the assumptions that lie behind our theoretical treatment, thus elucidating the contours of our approach. Next, we implement the LDA in order to derive explicit formulae solving the encounter problem. In section 3, we introduce the dynamic Monte Carlo algorithm and test it in the ideal case. Finally, in section 4, we present the numerical simulations for the purely repulsive and the attractive cases and compare the numerical results with our analytical predictions.

2. Accounting for excluded-volume and inter-particle interactions in the Smoluchowski theory

In this section we introduce our theoretical framework to include excluded-volume effects and inter-particle interactions in the theory of diffusion-limited bi-molecular encounters. For the sake of clarity, we start from the most general situation. Let us consider a fluid composed of $N = N_A +$

N_B interacting Brownian particles of type A and B, of radius a and b, and characterized by bulk densities and diffusivities ρ_A, D_A and ρ_B, D_B, respectively. The stochastic dynamics of the fluid is described by the N-body probability density $\mathcal{P}(\boldsymbol{x}_1, \boldsymbol{x}_2, \ldots, \boldsymbol{x}_{N_A}, \boldsymbol{y}_1, \boldsymbol{y}_2, \ldots, \boldsymbol{y}_{N_B}, t)$, where we have indicated with $\{\boldsymbol{x}_i\}$ and $\{\boldsymbol{y}_i\}$ the coordinates of the A and B particles, respectively. The probability P satisfies the full N-body Smoluchowski equation

$$\frac{\partial \mathcal{P}}{\partial t} = D_B \sum_{i=1}^{N_B} \vec{\nabla}_{y_i} \cdot \left[\vec{\nabla}_{y_i} \mathcal{P} + \beta \mathcal{P} \vec{\nabla}_{y_i} U_N \right] + D_A \sum_{i=1}^{N_A} \vec{\nabla}_{x_i} \cdot \left[\vec{\nabla}_{x_i} \mathcal{P} + \beta \mathcal{P} \vec{\nabla}_{x_i} U_N \right] \quad (6)$$

where $\beta^{-1} = k_B T$ and $U_N(\boldsymbol{x}_1, \boldsymbol{x}_2, \ldots, \boldsymbol{x}_{N_A}, \boldsymbol{y}_1, \boldsymbol{y}_2, \ldots, \boldsymbol{y}_{N_B})$ is the full N-body potential energy of the fluid.

Under the above hypotheses, we are thus finally led to the following effective one-body relative Smoluchowski equation

$$\frac{\partial \rho_1(\boldsymbol{r}, t)}{\partial t} = D \vec{\nabla} \cdot \left[\vec{\nabla} \rho_1 + \beta \left(\rho_1 \vec{\nabla} V + \int \rho_2(\boldsymbol{r}, \boldsymbol{r}', t) \vec{\nabla} v_2(\boldsymbol{r}, \boldsymbol{r}') \, \mathrm{d}^3 \boldsymbol{r}' \right) \right] \quad (7)$$

where $D = D_A + D_B$ is the relative diffusion coefficient. To recapitulate, in equation (7) $\boldsymbol{r}$ is the B–A vector, $V(\boldsymbol{r})$ is the B–A potential and $v_2(\boldsymbol{r}, \boldsymbol{r}')$ is the A–A potential. Furthermore, it will not be superfluous to recall that equation (7) is valid under the two following hypotheses:

H1 One species should be much more diluted than the other, namely $\rho_B \ll \rho_A$.

H2 The same species should be either static ($D_B = 0$, no size restriction) or diffusing much more slowly than the other ($D_B \ll D_A$, and consequently $b \gg a$).

In this study, we will restrict to the case $D_B = 0$. This setting is commonly referred to in the literature as the target problem, as it describes reactions between a particle in the dense fluid and an immobilized sink (the target).

2.1. Dynamical density functional theory and local density approximation

Equation (7) still presents significant difficulties, as the two-body density ρ_2 is not known. A possible way to proceed could be to opt for a mean-field-type factorization of the type $\rho_2(\boldsymbol{r}, \boldsymbol{r}', t) = \rho_1(\boldsymbol{r}, t)\rho_1(\boldsymbol{r}', t)$, as one does with the Bogolyubov–Born–Green–Kirkwood–Yvon or BBGKY hierarchy to obtain the Vlasov equation when also momenta are taken into account [15]. However, we will proceed here along a different route, which is more suitable to our aims. At equilibrium, the one-particle density of the A particle fluid is given by [15]

$$\rho_1(\boldsymbol{r}) = \Lambda^{-3} \exp\left[\beta \left(\mu - V(\boldsymbol{r})\right) + c_1(\boldsymbol{r})\right] \quad (8)$$

where Λ is the De Broglie thermal wavelength, μ is the total chemical potential and $c_1(\boldsymbol{r})$ is the two-body direct correlation function, whose physical meaning is to express all correlations between two particles except those that are mediated by single other particles. Equation (8) extends the known barometric law to the case of a fluid of pairwise interacting particles at equilibrium. Differentiation of equation (8) gives

$$\rho_1(\boldsymbol{r}) \vec{\nabla} c_1(\boldsymbol{r}) = \vec{\nabla} \rho_1(\boldsymbol{r}) + \beta \rho_1(\boldsymbol{r}) \vec{\nabla} V(\boldsymbol{r}) = -\beta \int \rho_2(\boldsymbol{r}, \boldsymbol{r}') \vec{\nabla} v_2(\boldsymbol{r}, \boldsymbol{r}') \, \mathrm{d}^3 \boldsymbol{r}'. \quad (9)$$

The last step follows by invoking the first equation in the known Yvon–Born–Green (YBG) hierarchy [16]. Note that this is consistent with the stationarity condition in equation (7). The direct correlation function can be computed at equilibrium from the functional derivative of the excess (with respect to the ideal fluid plus external potential) free-energy functional $\mathcal{F}_{ex}$ [15], namely

$$c_1(\boldsymbol{r}) = -\beta \frac{\delta \mathcal{F}_{ex}[\rho_1]}{\delta \rho_1} = \beta \mu_{ex}(\boldsymbol{r}), \quad (10)$$

where μ_{ex} denotes the corresponding excess chemical potential. Following the dynamical density functional theory (DDFT) approach of Marconi and Tarazona [17], we assume that the exact equilibrium closure that follows by combining equations (9) and (10) holds unchanged out of equilibrium, namely

$$\int \rho_2(\boldsymbol{r}, \boldsymbol{r}', t) \vec{\nabla} v_2(\boldsymbol{r}, \boldsymbol{r}') \, \mathrm{d}^3 \boldsymbol{r}' = \rho_1(\boldsymbol{r}, t) \vec{\nabla} \mu_{ex}(\boldsymbol{r}, t). \quad (11)$$

As a consequence, equation (7) becomes

$$\frac{\partial \rho_1(\boldsymbol{r}, t)}{\partial t} = D \vec{\nabla} \cdot \left[\vec{\nabla} \rho_1 + \beta \rho_1 \vec{\nabla} \left(V + \mu_{ex} \right) \right] \stackrel{\text{def}}{=} -\vec{\nabla} \cdot \vec{\mathcal{J}}_{YBG}. \quad (12)$$

We see that the excess chemical potential plays the role of an effective potential between the A particles and the B particle (the sink). Interestingly, we see that the DDFT hypothesis amounts to deriving a continuity equation for the one-particle density corresponding to a generalized current

$$\vec{\mathcal{J}}_{YBG} = -D \left[\vec{\nabla} \rho_1 + \beta \rho_1 \vec{\nabla} \left(V + \mu_{ex} \right) \right]. \quad (13)$$

More generally, equation (12) can be regarded as a DDFT extension of the time-dependent Smoluchowski equation for a non-ideal fluid. Under the aforementioned hypotheses H1 and H2, it can be employed to study the time-dependent encounter between two particles in a non-ideal fluid.

2.2. The encounter rate and the stationary density profile

In this work, we are not interested in the time-dependent problem, as we aim at calculating the encounter rate and the stationary one-particle density profile $\rho_1(\boldsymbol{r})$ for the non-ideal fluid of A particles. For the sake of clarity, we restrict ourselves here to the case $V = 0$, i.e. no external potential. Note that this strictly forbids to consider the case A = B, that is, encounter between identical particles in a monodisperse fluid. In fact, self-consistency would prescribe in this case $V(r) = v_2(r)$. In order to solve for the A–B encounter rate κ,

we integrate once the equation $\vec{\nabla}\cdot\vec{\mathcal{J}}_{\rm YBG}=0$ with the boundary conditions (3), which gives

$$\frac{\kappa}{4\pi Dr^2}=\frac{\partial\rho}{\partial r}+\beta\rho(r)\frac{\partial}{\partial r}\left[\mu_{\rm ex}(\{\rho\})\right], \tag{14}$$

where the integration constant κ is nothing but the encounter rate. Equation (14) can be integrated formally, to yield

$$\rho(r)=\left(\frac{\kappa}{\kappa_{\rm S}}\right)\rho_{\rm S}(r)-\beta\int_R^r\rho(r')\,\frac{{\rm d}\mu_{\rm ex}(r')}{{\rm d}r'}\,{\rm d}r', \tag{15}$$

where $\kappa_{\rm S}$ and $\rho_{\rm S}(r)=\rho_\infty(1-R/r)$ are the Smoluchowski rate and density profiles, respectively.

In principle, the excess chemical potential depends on the density profiles $\rho(r)$ in a non-local fashion, reflecting the presence of many-body spatial correlations [18]. In the spirit of the local density approximation (LDA), we assume that changes in the chemical potential at a certain position are only determined by the local density, that is, $\mu_{\rm ex}(r)=\mu_{\rm ex}(\rho(r))$. As a direct consequence of this approximation, one can transform the integration on r into a thermodynamic integration on the density. If we introduce the r-dependent and bulk packing fractions, $\phi(r)=4\pi a^3\rho(r)/3$ and $\phi_\infty=\lim_{r\to\infty}\phi(r)=4\pi a^3\rho_\infty/3$, we obtain the following integro-differential equation for the stationary profiles:

$$\phi(r)=\left(\frac{\kappa}{\kappa_{\rm S}}\right)\phi_{\rm S}(r)-\beta\int_0^{\phi(r)}\phi'\,\frac{{\rm d}\mu_{\rm ex}(\phi')}{{\rm d}\phi'}\,{\rm d}\phi'. \tag{16}$$

Taking the limit $r\to\infty$ of equation (16), one can derive the expression for the rate as a function of the packing fraction

$$\left(\frac{\kappa}{\kappa_{\rm S}}\right)=1+\frac{\beta}{\phi_\infty}\int_0^{\phi_\infty}\phi'\,\frac{{\rm d}\mu_{\rm ex}(\phi')}{{\rm d}\phi'}\,{\rm d}\phi'. \tag{17}$$

Using a standard thermodynamic relation between the excess chemical potential $\mu_{\rm ex}$ and the compressibility factor $Z(\phi)$ of the fluid (appendix B)

$$Z(\phi_\infty)=1+\frac{\beta}{\phi_\infty}\int_0^{\phi_\infty}\phi'\,\frac{{\rm d}\mu_{\rm ex}(\phi')}{{\rm d}\phi'}\,{\rm d}\phi' \tag{18}$$

the reaction rates and the density profiles can be reduced to

$$\frac{\kappa}{\kappa_{\rm S}}=Z(\phi_\infty) \tag{19a}$$

$$\frac{\phi(r)}{\phi_{\rm s}(r)}=\frac{Z(\phi_\infty)}{Z(\phi(r)).} \tag{19b}$$

Equations (19*a*) and (19*b*) are the main analytical results of the present communication. Interestingly, within the local density approximation, the gradient of the excess chemical potential can be rewritten as

$$\frac{\partial\mu_{\rm ex}(\rho(r))}{\partial r}=\frac{\partial\mu_{\rm ex}}{\partial\rho}\frac{\partial\rho}{\partial r}$$

and relation (14) as

$$\frac{\kappa}{4\pi D_0r^2}=\frac{{\rm d}\rho}{{\rm d}r}\left(1+\beta\rho(r)\frac{{\rm d}\mu_{\rm ex}}{{\rm d}\rho}\right), \tag{20}$$

where we have introduced D_0, the self-diffusion coefficient at infinite dilution. Using the thermodynamic relation

$$\beta\frac{{\rm d}\Pi}{{\rm d}\rho}=1+\beta\rho\frac{{\rm d}\mu_{\rm ex}}{{\rm d}\rho} \tag{21}$$

that stems directly from equation (18) and from the definition of the compressibility factor $Z(\phi)\rho=\beta\Pi(\rho)$, one can rewrite equation (14) for the steady-state Smoluchowski equation as

$$\frac{\kappa}{4\pi r^2}=D_0\frac{{\rm d}\rho}{{\rm d}r}\frac{\rm d}{{\rm d}\rho}[\beta\Pi(\rho)]\equiv D(\rho)\frac{{\rm d}\rho}{{\rm d}r}. \tag{22}$$

Therefore, within LDA the effect of self-crowding can be equivalently accounted for through an excess chemical potential that plays the role of an effective potential between the diffusing particle and the sink or via a density-dependent collective diffusion coefficient of the form $D(\rho)=D_0\,{\rm d}[\beta\Pi(\rho)]/{\rm d}\rho$ as used in a precedent study [19]. The LDA gives then the correct framework to justify formally the approach followed in [19].

3. Simulation scheme

In order to test the validity of the LDA we introduce an alternative to the event-driven Brownian dynamics (EDBD) [20, 21] scheme used in [10]—a dynamic Monte Carlo approach that makes it possible to study diffusing particles that have attractive interactions in addition to their hard-core repulsion.

The use of a different simulation scheme, however, is a delicate issue. For EDBD, we have shown that the choice of the time step would alter profoundly the nature of the Smoluchowski process simulated [10]. If the time step is too large, deviations can be strong as the absorption process becomes dependent on inertial effects[7]. In particular, we have shown in [10] that for large time steps EDBD reproduces the results of the full (underdamped) Fokker–Planck dynamics. This validation was a necessary step, required to control possible artefacts resulting from the type of time integrator chosen in the numerical simulations. For a dynamic Monte Carlo, a similar validation in the framework of an encounter reaction process is also necessary and will be discussed in section 3.1.

3.1. Dynamic Monte Carlo (DMC)

The simulation set-up consists of a cubic box with periodic boundary conditions. Reactants of radius a are initially placed uniformly inside the box and let diffuse. When a particle encounters the sink, a sphere of radius b located at the centre of the box, it is absorbed and consequently reinserted in a buffering layer at the box edges. The reinserted particles are immobilized in the buffering layer until their overlap with neighbouring diffusers vanish. To speed up the reinsertion process, a repulsive interaction between the diffusers and the

[7] We address inertial effects on bi-molecular encounters in detail in a separate paper.

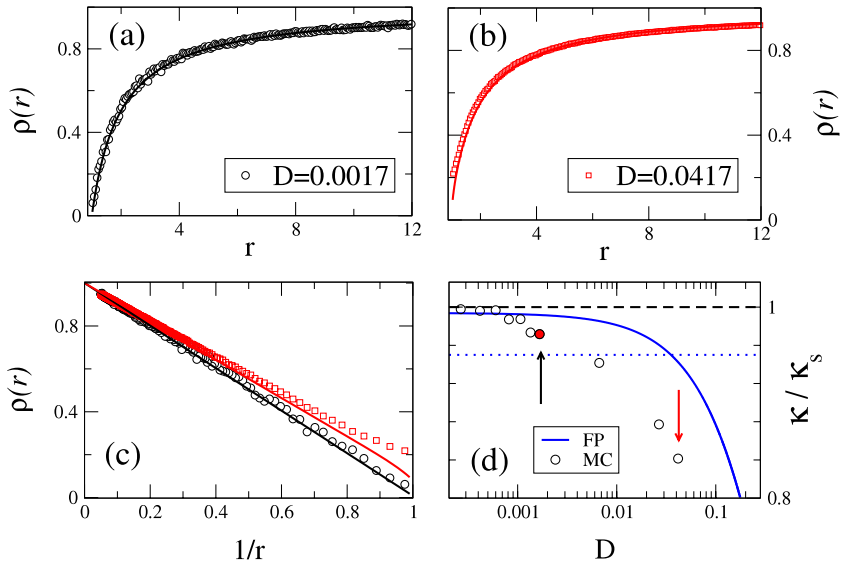

Figure 1. Simulated density profiles (top and bottom left panels, symbols) and reaction rates (bottom right panel, symbols) of ideal (non-interacting) diffusers as a function of the bare diffusivity $D_0 = \frac{1}{6}\Delta r^2$ compared to the corresponding Fokker–Planck (FP) solutions (lines). For sufficiently small Δr the dynamic Monte Carlo simulations (DMC) are in perfect agreement with the Fokker–Planck solution and the overdamped Smoluchowski density profile $\rho_s(r)$ and reaction rate κ_s are recovered. The arrows mark explicitly the values of D_0 corresponding to the reported density profiles. The filled symbol corresponds to $\Delta r = 0.1$ which has been used in the rest of the paper. The horizontal dotted line corresponds $\kappa/\kappa_s = 0.95$.

reinserted particles is added. This reinsertion process ensures, after a suitable transient, constant-flux boundary conditions. Particles moves are accepted according to standard Metropolis criteria with displacement Δr and an acceptance rate $\mathrm{ac}(\Delta r)$.

In the dynamic Monte Carlo scheme, an MC cycle is converted into real time as proposed in [22, 23]. We consider a cycle as an attempt to move N particles by standard Monte Carlo (MC), N being the total number of particles. In this case, we can use the conversion rate

$$\Delta\tau = \frac{\Delta t}{\text{cycle}} = \frac{\Delta r^2\ \mathrm{ac}(\Delta r)}{6D_0} \tag{23}$$

where $\mathrm{ac}(\Delta r)$ is the average acceptance rate, D_0 the infinite dilution diffusion constant and Δr is the maximum displacement. For a sufficiently small Δr, one Monte Carlo step corresponds to the time given by the acceptance ratio $\mathrm{ac}(\Delta r)$ [22, 23].

3.1.1. Non-interacting ideal diffusers. As first validations of the dynamical Monte Carlo scheme for diffusion reaction, we computed the encounter rate and density profile for the ideal case. In this case, all Monte Carlo moves are accepted since the particles are simply point-like, therefore $\mathrm{ac}(\Delta r) = 1$. The diffusivity $D_0 = \frac{1}{6}\Delta r^2$ of the particles is controlled by changing the maximum displacement Δr that can be given to a particle at each Monte Carlo move [22, 23]. In this way one can probe the reaction rate and density profiles from underdamped conditions down to the purely diffusive Smoluchowski regime. We have shown recently that inertial effects can play an important role if the dynamics is not completely overdamped [10], in agreement with the Fokker–Planck (FP) solution of the Smoluchowski problem derived by Harris [24].

The density profiles are presented for two representative Δr in figure 1. In the limit where Δr is small compared to the typical distance in the system ($\simeq a + b$), the overdamped Smoluchowski regime holds and the Smoluchowski density profile, equation (4), is perfectly reproduced by our dynamical Monte Carlo scheme, as presented in figures 1(a)–(c). For larger Δr the agreement between the Monte Carlo results and the Smoluchowski solutions is less satisfactory (see figure 1(d)).

In figure 1(d), we also present the results for the ratio between the numerically computed reaction rate and the ideal rate κ_S, equation (5), for different values of D_0. Recently, we have shown that inertial effects can play an important role, if the dynamics is not completely overdamped [19]. This can be seen by comparing the Fokker–Planck (FP) solution of Smoluchowski problem [24] with the numerical results equation, also shown in figure 1(c). For a short enough MC step, the numerical results effectively reproduce the Smoluchowski rate with an accuracy below 5%. For larger values of Δr, however, the numerical rate is smaller than in the ideal case and does not follow the FP solution. This is an important difference with respect to our previous event-driven Brownian dynamics (EDBD) results, which showed a better agreement with the FP solution. In the present paper we are not interested in inertial effects. In cases where these effects are relevant, different theoretical approaches may be followed, such as the one recently proposed in [25].

Summarizing, provided Δr is small enough, we can use the dynamic MC scheme to investigate numerically the reaction rates. For all the results presented in the rest of the paper, dynamic MC has been used with $\Delta r = 0.1$ which is represented by a filled symbol in figure 1(d).

4. Numerical tests of the local density approximation

In this section, we want to test the results of the solution of the DDFT equations within the LDA approximation presented in equations (19*a*) and (19*b*) for the Smoluchowski stationary problem. The main strength of these equations is the fact that we can express the stationary density profile and the reaction rate in terms of an equation of state (EOS). This result should provide a first improvement on the ideal case, equations (4) and (5), and we shall test this correction with the help of numerical simulations for two different model systems. The first model will be purely repulsive while the second one will present some attractive interactions.

For the purely repulsive case, we investigate the simple hard sphere model (HSM). This model has been widely used in this context and we have also used it before [10]. For the HSM, we will use the Carnahan–Starling (CS) EOS that has been proved to be reliable up to significantly high densities.

For the attractive case, we used the square well (SW) model with a short-ranged interaction. The properties of SW fluids can be well described using the optimized equation of state based on a fourth-order free-energy expansion introduced in [27].

4.1. Hard sphere case

In a previous study we inferred the density dependence of the rate $\kappa/\kappa_S = Z(\phi_\infty)$ equivalent to equation (19*a*) by introducing an effective density-dependent mobility in the single-particle Smoluchowski equation [10] and compared it with the results of event-driven Brownian dynamics simulations for hard sphere diffusers, finding excellent agreement with the numerics for $b \gg a$. We have shown above that the LDA results are equivalent to the one obtained by this effective density-dependent mobility. The use of the DDFT, however, comes from first-principle considerations and it can be the base for future extensions that could possibly go beyond LDA. For this reason, we will discuss again the case of HS here. There is also another reason to discuss again the rate of HS. Since dynamic Monte Carlo is a completely different approach with respect to event-driven Brownian dynamics, we can use the rate of the theory, that already proved to be quantitatively correct, as a stringent test of its validity.

Looking at figure 2(b), it is evident that the reaction rate for a system with $b = 1$ and $a = 1/2$ does increase according to the compressibility factor $Z(\phi)$ of the hard sphere solution, as expected from the LDA derivation and the EDBD simulations of [10]. For $b \leq a$, the rate was found to saturate and to become even a nonmonotonic function of ϕ concurrently to the emergence of spatial oscillations in the density profile that set in near the sink [10]. The description of this particular regime would require a theory beyond the LDA, incorporating a non-local coupling between the density and the local excess chemical potential. This is beyond the scope of the present paper.

More interesting is the comparison between of the LDA predictions with the numerical results. To this aim, the LDA density profile were obtained solving numerically

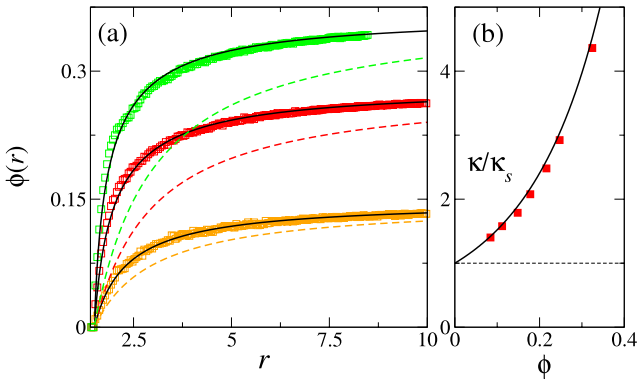

Figure 2. Density profiles $\phi(r)$ (a) and reaction rate κ/κ_S (b) for mixtures of hard sphere particles ($b = 1$, $a = 1/2$) as a function of their packing fraction ϕ. (a) From top to bottom: $\phi = 0.351, 0.275$ and 0.149. The solutions of equations (19*a*) and (19*b*) (solid lines) are compared with the dynamic Monte Carlo simulations (symbols) and with the Smoluchowski density profiles $\phi_S(r)$ and reaction rate κ_S (dashed lines).

equation (19*b*) with the CS equation of state as input. Figure 2(a) shows that LDA provides an excellent description of the distribution of diffusing particles around the absorbers, at least up to $\phi = 0.35$,[8] and it improves significantly over the Smoluchowski result, i.e. equation (4). At higher packing, density structuration emerges at short distances from the absorber for the size ratio $b/a = 2$ considered here, in agreement with our previous observations [10]. The packing fraction at which non-local effects emerge is not easy to be determined *a priori* and depends on the size ratio between the reactants and the sink. The size ratio discussed in this paper guarantees that the LDA is substantially correct for a large range of densities where crystallization or kinetic arrest might play a relevant role. These densities. however, are well above the typical crowding conditions that are encountered in biological conditions. The new solution tends to saturate more rapidly than the ideal case (dashed lines in figure 2(a)) to the bulk value. This suggests the existence of a decoupling of the sink and bulk regions with respect to the non-interacting case. Long-range correlations induced in the whole fluid by the presence of a local absorbing region are more rapidly quenched away from the sink when increasing the bulk density. These numerical results for hard sphere particles confirm the ones presented in [10] and demonstrate the validity of the LDA for the description of both the reaction rate and the density profile in a crowded environment of hard sphere diffusers that are competing to reach a spherical target of large size.

4.2. Square well case

In order to test further the range of validity of the LDA approach and as a first step towards the case of diffusing particles with more general interactions encountered in biological systems or colloidal suspensions, we extend this study to particles with attractive interactions. We implemented

[8] We drop the $_\infty$ subscript for the sake of clarity.

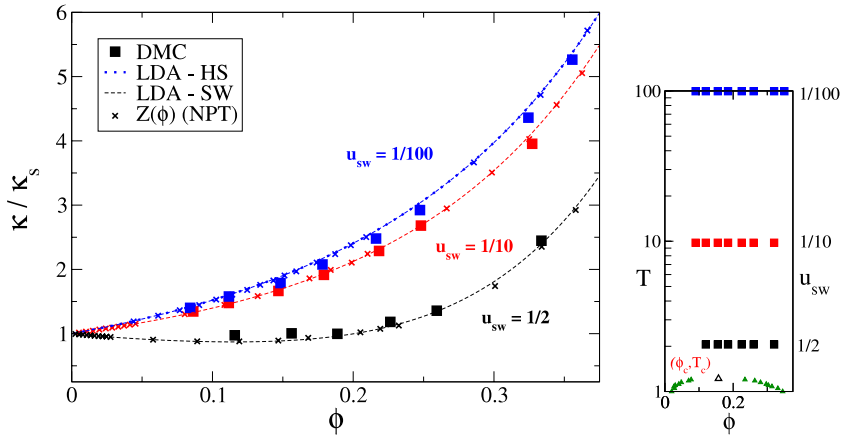

Figure 3. Left panel: reaction rate for mixtures of square well diffusers as a function of their packing fraction ϕ and attraction strength $u_{\rm sw}$. The DMC results (filled symbols) follow closely the $(\phi, u_{\rm sw})$ dependence of the rate as predicted by equation (19*a*) (lines), thus validating the LDA description of the reaction rate for a large range of density and stickiness of the diffusers. The compressibility factors computed from the Carnahan–Starling equation of state for hard spheres (dotted lines) and from the optimized EOS of [27] for square well interactions (dashed lines) are shown together with the results of isobaric NPT simulations (crosses). Right panel: liquid–gas coexistence curve and critical point of the square well model used to model the attraction between the diffusers (triangles from [28]). Other parameters are: $a = 1$, $b = 1/2$ and $\Delta r = 0.1$.

the DMC scheme to compute the reaction rate of SW diffusers. The interaction potential of additive hard sphere particles with short-range SW interaction is defined as

$$\frac{U(r)}{k_{\rm B}T} = \begin{cases} \infty & \text{if } x < d \\ -u_{\rm sw} & d < x < \lambda\, d \\ 0 & x > \lambda\, d, \end{cases} \qquad (24)$$

with $d = 2a = 1$. $u_{\rm sw}$ and λ define the strength and the range of the interaction respectively. In the following the interaction strengths $u_{\rm sw}$ will be expressed in units of $k_{\rm B}T$ and distances in units of $d = 1$. The temperature is fixed to unity, $T = 1$. The liquid-gas critical point for the square well particles of range $\lambda = 1.5$ investigated here is located at $(\phi_c, T_c) = (0.157, 1.219)$ [28], corresponding to an interaction strength of $u_{\rm sw} = 1/1.219$. We studied this mixture for attraction strengths ranging from the hard sphere high-temperature limit ($u_{\rm sw} = 1/100$) down to temperatures close to the critical one ($u_{\rm sw} = 1/2$). In order to solve equations (19*a*) and (19*b*) to compute respectively the LDA reaction rate and the density profile, the only input is an EOS for the SW. In the present work, we opted for an optimized equation of state for square well fluid based on a fourth-order free-energy expansion that has been introduced recently [27]. Before using this result for the reaction problem, we tested it by Monte Carlo simulation results obtained in the isobaric ensemble (NPT). We calculate $Z(\phi)$ for the interactions strengths we are interested in and for several densities. The results are presented in figure 3. This optimized EOS is manifestly highly accurate in the density and temperature regime of interest in this study.

The good agreement between the LDA results and the DMC numerical simulation for the reaction rate for attractive particles is also illustrated by figure 3. As expected, for weak attractions, results similar to those obtained for HS are recovered. In fact, the ratio $\kappa/\kappa_{\rm S}$ increases monotonically with packing fraction. For stronger coupling, i.e. $u_{\rm sw} = 1/2$, the effect of the inter-particle attraction becomes relevant. The reduced rate no longer grows monotonically, but presents a weak decrease until $\phi = 0.2$ and then it grows again. We can conclude that the attraction among the diffusers counterbalances the steric effects and, in the present case, there is a large interval of packing fractions in which the non-ideal rate does not depart significantly from the ideal case. The LDA appears to hold also in the case of 'sticky' diffusers and the reaction rate of attractive reactants to be governed by their compressibility factor for a large range of density and 'stickiness' conditions, in agreement with equation (19*a*).

We used the same EOS to solve the non-linear equation (19*b*) for the density profile derived within the LDA. In this case we focused on two attractive cases, $u_{\rm sw} = 1/2, 1/5$, where the effect of attraction is relevant. As illustrated in figure 4, the LDA provides a very good description of the Monte Carlo results for a large range of attraction strengths and packing fractions. We note that by increasing the stickiness of the particles, the system retains memory of the sink on a larger length scale, the density profile reaching a given density ρ^* further away from the absorber the larger is $u_{\rm sw}$.

5. Conclusions

In this paper we have developed an approach based on a local density approximation to describe diffusion-limited reactions occurring in a fluid of interacting particles. The chosen setting was the one commonly referred to as the target problem, i.e. encounter reactions occurring between a particle of the fluid and an immobilized sink (the target). A comparison of our analytical treatment with the simple case of spherical hard-core particles shows excellent agreement between theory and simulations. The agreement is expected to hold as long as the LDA holds, i.e. under the hypothesis that the size of

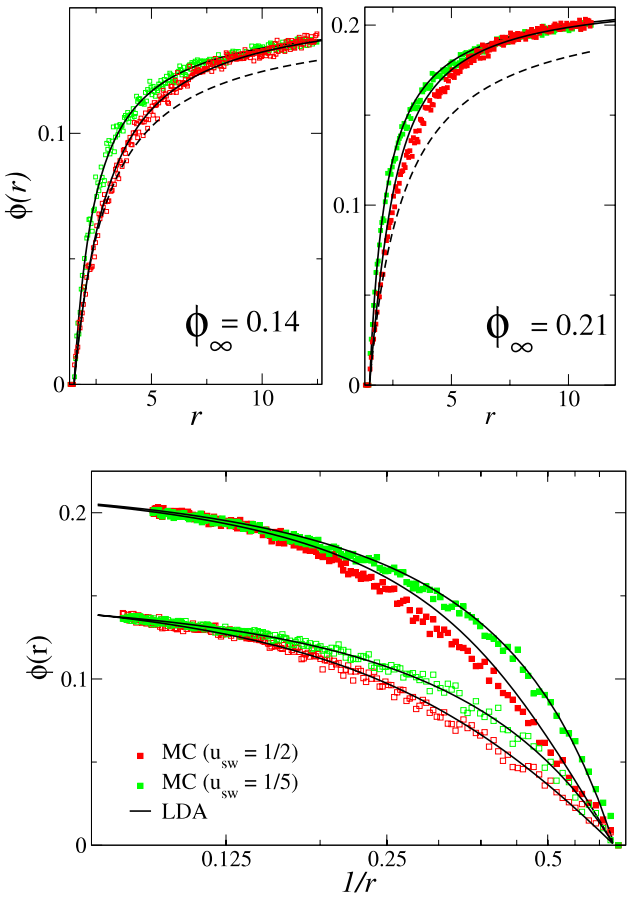

Figure 4. Density profiles for mixtures of square well diffusers as a function of their packing fraction ϕ and attraction strength u_{sw}. The density profiles obtained from DMC simulations (symbols) are in very good agreement with the numerical solution of equation (19*b*) (solid lines) derived within the LDA. The dashed lines are the Smoluchowski density profiles. Other parameters are: $a = 1$, $b = 1/2$ and $\Delta r = 0.1$.

the Brownian particles is much smaller than that of the sink. When this is not the case, oscillations in the stationary density profiles in the fluid around the sink set in and the rate no longer increases monotonically with the density [10]. This simple observation flags the emergence of correlations that we expect to play an important role. For example, it has been well recognized that at high densities crowding can be an important regulatory mechanism [29] and strongly alter the mechanical properties of the cell [30]. Another important source of correlation is represented by the nature of the local environment where a process occurs in the cell. For example, it has been recently argued that phase separation could be a fundamental mechanism for the structuration and compartmentalization of the cell [33]. While a lot has been understood at the experimental level, a viable theoretical approach still appears missing, as it is not an easy task to take into account correlations and local fluctuations. Another possible approach could be represented by kinetic theories. As a matter of fact, it can be shown that LDA and Enskog theory are equivalent [31]. This has been shown, for example, in the framework of sedimentation of hard spheres. However, it is clear that both approaches cannot go beyond a simple local description. This notwithstanding, it has been argued that this should not prevent them to describe crystallization in the case of sedimentation [32]. However, the character of locality has proved to be a limitation of the LDA and Enskog approximations. We expect that the improvement to the theory could be tackled both from DFT and from the Enskog theory, but, in this paper, we have discussed only the former in detail. In order to capture this effect, one needs to consider non-local coupling between the density and the local excess chemical potential. For systems of hard spheres, one way to do this would be to employ Rosenfeld's fundamental measure theory as a means to approximate the excess free-energy functional [34]. However, this route may prove extremely computationally demanding and certainly falls beyond the scope of the present paper.

Another important aspect that has been neglected in the present context is the role of hydrodynamic interactions. As a matter of fact, hydrodynamics has been recently shown to play an important role in diffusion-related processes occurring in crowded conditions [9]. The role of hydrodynamics is indeed beyond the scope of the present paper. However, effective computational and theoretical tools exist that could be employed to this aim, such as those introduced recently in [26, 35]. The goal of the present study was to develop and test a novel analytic approach to describe the encounter rate within a dense fluid. Therefore, we limited the study to regions in the temperature–density plane that could be accounted for precisely by the optimized equation of state required as input in LDA approach. However, we would like to stress that the present study could be effortlessly extended to investigate numerically the effects on the reaction rate of density fluctuations that appear in the close vicinity of the liquid–vapour critical point. The dynamical Monte Carlo scheme could indeed be used in that regime. From a practical perspective, a different potential of interaction in terms of range or shape might be more suited to avoid crystallization in the system at high densities and low temperatures.

Another promising numerical experiment would be to cool down the solution of diffusing agents below its critical temperature and thus study the effect of phase separation on the reaction rate. The difficulty would be here to simulate in a meaningful way this non-equilibrium system. But this might be particularly relevant as a first step to characterize the influence of phase separation on reaction rate in colloidal suspension or biochemical reactions in general.

In summary, our theoretical framework allows one to compute encounter rates and stationary density profiles in crowded media in the target approximation under a wide range of conditions. Moreover, it provides a coherent reading frame where to accommodate additional features for investigating more realistic systems, including, e.g., complex inter-particle potentials with attractive and repulsive forces and reactions between molecules of different species.

Acknowledgments

FP gratefully acknowledges financial support from the Swiss National Science Foundation under the Short scientific

visits scheme for his visit to EPFL, where part of this work has been carried out (IZK0Z2_137475). ND acknowledges support SNSF (Project no. PBELP2_130895) and ERC (Advanced Grant 227758), CDM by ERC (226207-PATCHYCOLLOIDS), SNSF (visiting grant IZK022_121268). GF acknowledges support by the SNSF (grants PP0022_119006 and PP0022_140822/1). The authors would like to thank A Szabo for enlightening discussions. We also thank Allen Minton for interesting discussions.

Appendix A. Derivation of one-body relative Smoluchowski equation (equation (7))

In principle, equation (6) could be solved to calculate the rate of bi-molecular encounters between A and B particles. However, this is clearly impossible and some approximations are required [36, 37]. The first approximation needed is to assume that one of the two species (say B) is much more diluted than the other, i.e. $\rho_B \ll \rho_A$, so that B–B encounter events can be neglected on the typical timescales of A–A and A–B encounters. In this case, the problem can be considerably simplified by studying the encounter dynamics of an isolated B particles surrounded by a sea of N_A particles of type A (in the following we shall drop the A subscript for the sake of clarity). Hence, one has a reduced $(N+1)$-body Smoluchowski equation for the probability density $\mathcal{P}(\boldsymbol{y}, \{\boldsymbol{x}_1\}, t)$:

$$\frac{\partial \mathcal{P}}{\partial t} = D_B \vec{\nabla}_y \cdot \left[\vec{\nabla}_y \mathcal{P} + \beta \mathcal{P} \vec{\nabla}_y U_{N+1}\right] + D_A \sum_{i=1}^{N_A} \vec{\nabla}_{x_i} \cdot \left[\vec{\nabla}_{x_i} \mathcal{P} + \beta \mathcal{P} \vec{\nabla}_{x_i} U_{N+1}\right]. \quad (A.1)$$

We wish to stress that the above assumption appears as an almost necessary step, whatever the theoretical treatment of diffusion-limited bi-molecular reactions. The logical step at this point is to change coordinates to the rest-frame of the B particle, i.e. $\boldsymbol{r}_i = \boldsymbol{x}_i - \boldsymbol{y}$, so that

$$\nabla^2_{x_i} \longrightarrow \sum_{i,j} \nabla_{r_i} \cdot \nabla_{r_j}. \quad (A.2)$$

In the new coordinate system, equation (A.1) reads

$$\frac{\partial P}{\partial t} = (D_A + D_B) \sum_{i=1}^{N} \vec{\nabla}_i \cdot \left[\vec{\nabla}_i P + \beta P \vec{\nabla}_i \mathcal{U}\right] + D_B \sum_{i=1}^{N} \sum_{j \neq i} \vec{\nabla}_i \cdot \left[\vec{\nabla}_j P + \beta P \vec{\nabla}_j \mathcal{U}\right], \quad (A.3)$$

where we have defined $P = \int \mathcal{P}\, \mathrm{d}^3\boldsymbol{y}$, $\mathcal{U} = U_{N+1}(\boldsymbol{r}_1, \boldsymbol{r}_2, \ldots, \boldsymbol{r}_N)$ and it is intended that the differential operators act on the new relative coordinates $\{\boldsymbol{r}\}$. As it has been already remarked by Szabo [3], the surprising result is that, even if equation (A.3) describes the relative diffusion of N particles A in the rest-frame of an isolated B particle, the motion of the latter causes the appearance of nasty cross-terms, that vanish only in the limit of a stationary B, i.e. in the context of the target problem.

We turn now to deriving the appropriate one-particle Smoluchowski equation from the full N-body problem. The standard procedure is to assume that the N-body potential energy $\mathcal{U}$ may be expressed in terms of a two-body potential acting on each B–A pair (an external potential for the fluid of A particles), $V(\boldsymbol{r}_i)$ and that the A–A interactions can be accounted for by a sum of pair potentials $v_2(\boldsymbol{r}_i, \boldsymbol{r}_j)$, three-body potentials $v_3(\boldsymbol{r}_i, \boldsymbol{r}_j, \boldsymbol{r}_k)$ and higher-order interactions [36],

$$\mathcal{U} = \sum_{i=1}^{N} V(\boldsymbol{r}_i) + \tfrac{1}{2} \sum_{i=1}^{N} \sum_{j \neq i} v_2(\boldsymbol{r}_i, \boldsymbol{r}_j) + \tfrac{1}{6} \sum_{i=1}^{N} \sum_{j \neq i} \sum_{k \neq j \neq i} v_3(\boldsymbol{r}_i, \boldsymbol{r}_j, \boldsymbol{r}_k) + \cdots. \quad (A.4)$$

Correspondingly, we introduce the one-body, two-body and k-body densities

$$\begin{aligned} \rho_1(\boldsymbol{r}_1, t) &= N \int \mathrm{d}^3\boldsymbol{r}_2 \cdots \int \mathrm{d}^3\boldsymbol{r}_N\, P(\{\boldsymbol{r}\}, t) \\ \rho_2(\boldsymbol{r}_1, \boldsymbol{r}_2, t) &= N(N-1) \int \mathrm{d}^3\boldsymbol{r}_3 \cdots \int \mathrm{d}^3\boldsymbol{r}_N\, P(\{\boldsymbol{r}\}, t) \\ &\ldots \\ \rho_k(\boldsymbol{r}_1, \boldsymbol{r}_2, \ldots, \boldsymbol{r}_k, t) &= \frac{N!}{(N-k)!} \int \mathrm{d}^3\boldsymbol{r}_{k+1} \cdots \int \mathrm{d}^3\boldsymbol{r}_N\, P(\{\boldsymbol{r}\}, t). \end{aligned} \quad (A.5)$$

In order to derive the effective one-body Smoluchowski equation, one should substitute the expansion (A.4) into equation (A.3) and integrate over $N-1$ degrees of freedom with the requirement that the terms of the type $\int \partial P/\partial \boldsymbol{r}_j \ldots \mathrm{d}^3\boldsymbol{r}_j$ yield a vanishing contribution [15]. We will report the result in the approximation of pairwise-only interaction, i.e. $v_k = 0$ for $k > 2$. After some lengthy but rather straightforward algebra, we get

$$\begin{aligned} \frac{\partial \rho_1(\boldsymbol{r}, t)}{\partial t} &= (D_A + D_B) \times \vec{\nabla} \cdot \left[\vec{\nabla}\rho_1 + \beta\left(\rho_1 \vec{\nabla} V + \int \rho_2(\boldsymbol{r}, \boldsymbol{r}', t) \vec{\nabla} v_2(\boldsymbol{r}, \boldsymbol{r}')\, \mathrm{d}^3\boldsymbol{r}'\right)\right] \\ &+ \beta D_B \left[\vec{\nabla} \cdot \int \rho_2(\boldsymbol{r}, \boldsymbol{r}', t) \vec{\nabla}' V(\boldsymbol{r}')\, \mathrm{d}^3\boldsymbol{r}' \right. \\ &+ \vec{\nabla} \cdot \int \rho_3(\boldsymbol{r}, \boldsymbol{r}', \boldsymbol{r}'', t) \vec{\nabla}' v_2(\boldsymbol{r}', \boldsymbol{r}'')\, \mathrm{d}^3\boldsymbol{r}'\, \mathrm{d}^3\boldsymbol{r}'' \\ &\left. + \int \rho_3(\boldsymbol{r}, \boldsymbol{r}', \boldsymbol{r}'', t) \vec{\nabla}' \cdot \vec{\nabla}'' v_2(\boldsymbol{r}', \boldsymbol{r}'')\, \mathrm{d}^3\boldsymbol{r}'\, \mathrm{d}^3\boldsymbol{r}''\right], \end{aligned} \quad (A.6)$$

where superscripts in the nabla operators denote differentiation with respect to the corresponding superscripted variables. We note that, despite the pairwise approximation for the inter-particle interactions, the cross-terms caused by the motion of the target B particle generate three-body terms in the effective one-body Smoluchowski equation. We see that, in order to come up with a tractable equation, one is led to a further assumption, namely $D_B \ll D_A$. Not only do the B particles have to be much less densely distributed, but they should also

diffuse much more slowly than the A particles. This amounts of course to the equivalent size restriction $b \gg a$.

Appendix B. Compressibility factor from the chemical potential (equation (18))

Here we derive equation (18) following the route described by Widom [38]. The compressibility factor $Z(\phi)$ can be directly computed as

$$Z = \phi \left(\frac{\mathrm{d}}{\mathrm{d}\phi} \left(\frac{\beta F}{N} \right) \right)_{T;N}. \tag{B.1}$$

Performing a thermodynamic integration on $[0, \phi]$ of equation (B.1) we get the excess free-energy

$$\frac{\beta F^{\mathrm{ex}}(\phi)}{N} = \int_0^{\phi} \frac{Z-1}{\phi'} \mathrm{d}\phi'. \tag{B.2}$$

From F^{ex}, we can derive the excess chemical potential

$$\beta \mu^{\mathrm{ex}} = \frac{\beta F^{\mathrm{ex}}}{N} + (Z-1). \tag{B.3}$$

From equation (B.2), one has

$$\beta \mu^{\mathrm{ex}}(\phi) = \int_0^{\phi} \frac{Z(\phi)-1}{\phi'} \mathrm{d}\phi' + (Z(\phi)-1). \tag{B.4}$$

This equation can be inverted by multiplying both sides by ϕ and then differentiating with respect to ϕ. One thus gets

$$\beta \phi \frac{\mathrm{d}\mu^{\mathrm{ex}}}{\mathrm{d}\phi} = \frac{\mathrm{d}}{\mathrm{d}\phi} \left[\phi (Z-1) \right]. \tag{B.5}$$

Finally, equation (18) is obtained through a simple thermodynamic integration.

References

[1] Keizer J 1987 *Chem. Rev.* **87** 167
[2] Smoluchowski M V 1916 *Z. Phys. Chem.* **92** 129
[3] Szabo A 1989 *J. Chem. Phys.* **93** 6929
[4] Zhou H-X, Rivas G and Minton A P 2008 *Annu. Rev. Biophys.* **37** 375–97
[5] Dix J A and Verkman A S 2008 *Annu. Rev. Biophys.* **37** 247–63
[6] Elcock A H 2010 *Curr. Opin. Struct. Biol.* **20** 196
[7] Reiss H, Frisch H L and Lebowitz J L 1959 *J. Chem. Phys.* **31** 369
[8] Cheung M S, Klimov D and Thirumalai D 2005 *Proc. Natl Acad. Sci. USA* **102** 4753
[9] Ando T and Skolnick J 2010 *Proc. Natl Acad. Sci. USA* **107** 18457
[10] Dorsaz N, De Michele C, Piazza F, De Los Rios P and Foffi G 2010 *Phys. Rev. Lett.* **105** 120601
[11] Jiao M, Li H T, Chen J, Minton A P and Liang Y 2010 *Biophys. J.* **99** 914
[12] Miklos A C, Sarkar M, Wang Y and Pielak G J 2011 *J. Am. Chem. Soc.* **133** 7116
[13] Rosen J, Kim Y C and Mittal J 2011 *J. Phys. Chem.* B **115** 2683
[14] Feig M and Sugita Y 2012 *J. Phys. Chem.* B **116** 599
[15] Hansen J-P and McDonald I R 2006 *Theory of Simple Liquids* (London: Academic)
[16] Rowlinson J S and Widom B 1982 *Molecular Theory of Capillarity* (Oxford: Clarendon)
[17] Marconi U M B and Tarazona P 1999 *J. Chem. Phys.* **110** 8032
[18] Rosenfeld Y, Levesque D and Weis J-J 1990 *J. Chem. Phys.* **92** 6818
[19] Dorsaz N, De Michele C, Piazza F and Foffi G 2010 *J. Phys.: Condens. Matter* **22** 104116
[20] Scala A, Voigtmann Th and De Michele C 2007 *J. Chem. Phys.* **126** 134109
[21] De Michele C 2010 *J. Comput. Phys.* **229** 3276
[22] Sanz E and Marenduzzo D 2010 *J. Chem. Phys.* **132** 194102
[23] Romano F, De Michele C, Marenduzzo D and Sanz E 2011 *J. Chem. Phys.* **135** 124106
[24] Harris S 1982 *J. Chem. Phys.* **77** 934
[25] Marconi U M B and Melchionna S 2007 *J. Chem. Phys.* **126** 184109
[26] Gompper G, Ihle T, Kroll K and Winkler R G 2009 *Adv. Polym. Sci.* **221** 1
[27] Espíndola-Heredia R, del Río F and Malijevsky A 2009 *J. Chem. Phys.* **130** 024509
[28] Vega L, de Miguel E and Rull L F 1992 *J. Chem. Phys.* **96** 2296
[29] Miermont A, Waharte F, Hu S, McClean M N, Bottani S, Lon S and Hersen P 2013 *Proc. Natl Acad. Sci. USA* **110** 5725
[30] Zhou E H, Trepa X, Park C Y, Lenormand G, Oliver M N, Mijailovich S M, Hardinc C, Weitz D A, Butler J P and Fredberg J J 2009 *Proc. Natl Acad. Sci. USA* **106** 10632–7
[31] Levin Y 2000 *Physica* A **287** 100
[32] Quinn P V and Hong D C 2000 *Phys. Rev.* E **62** 8295
[33] Miermont A, Waharte F, Hu S, McClean M N, Bottani S, Lon S and Hersen P 2012 *Cell* **149** 1188
[34] Rosenfeld Y 1989 *Phys. Rev. Lett.* **63** 980
[35] Marconi U M B and Melchionna S 2009 *J. Chem. Phys.* **131** 014105
[36] Archer A J and Evans R 2004 *J. Chem. Phys.* **121** 4246
[37] Archer A J and Rauscher M 2004 *J. Phys. A: Math. Gen.* **37** 9325
[38] Widom B 1963 *J. Chem. Phys.* **39** 2808